JOURNAL OF PROPULSION AND POWER
Vol. 11, No. 1, January–February 1995

Wave Rotor Charging Process: Effects of Gradual Opening and Rotation

L. M. Larosiliere*
Ohio Aerospace Institute, Cleveland, Ohio 44135

The wave rotor charging process under conditions of gradual opening accompanied by passage rotation is numerically simulated. Insights into the response of the interface and kinematics of the flowfield to various opening times are given. Since the opening time is inversely proportional to the rotational speed of the rotor, effects of passage rotation such as centripetal and Coriolis accelerations are intrinsically coupled to the gradual opening process. Certain three-dimensional features associated with the charging process as a result of centripetal and Coriolis accelerations are illustrated. It is shown that the interface between driver and driven gas acquires a three-dimensional distortion depending on the rotational speed and opening time.

Nomenclature

a	=	speed of sound
B	=	dimensionless ratio of time scales
E	=	total energy per unit mass
$\hat{e}$	=	unit vector
h_{tR}	=	rothalpy
L	=	passage length
Mo, M_Ω	=	wheel Mach number based on tip radius and a reference speed of sound
p	=	pressure
R_H	=	hub radius
R_T	=	tip radius
R_Ω	=	rotation parameter
T	=	temperature
t	=	time
w	=	relative velocity vector
γ	=	ratio of specific heats
θ	=	azimuthal coordinate in a stationary reference frame
θ'	=	azimuthal coordinate on the rotating passage
ρ	=	density
τ	=	reference time scale
Φ	=	passage sector angle
Ω	=	rotational speed

Subscripts

L	=	longitudinal direction
o	=	passage opening
∞	=	uniform reference state, defined in text
Ω	=	axis of rotation

Introduction

CONCEPTUALLY, a wave rotor is based on the idea of energy exchange between two fluid streams by way of unsteady waves. Wave rotor machines typically consist of several cylindrical passages mounted along the periphery of a steadily rotating drum. Each of these passages is cyclically exposed to different end conditions that generate unsteady waves for energy transfer. The development and application of wave rotor machines are extensively reviewed in Ref. 1.

Presented as Paper 93-2526 at the AIAA/SAE/ASME/ASEE 29th Joint Propulsion Conference and Exhibit, Monterey, CA, June 28–30, 1993; received July 19, 1993; revision received Feb. 26, 1994; accepted for publication March 2, 1994.

*Senior Research Associate, NASA Lewis Research Center. Member AIAA.

Figure 1 illustrates a typical wave rotor charging process. The passage initially contains a quiescent fluid with pressure and temperature smaller than those of the inlet-port stream. If the passage were to instantaneously open to the port conditions, fluid would rush in and initiate a rightward moving shock wave followed by a contact interface separating driver fluid from driven fluid. When the primary shock reaches the right wall, a postcompression shock is generated causing the driven fluid to be at a higher pressure than that of the inlet-port stream. In a practical rotor, the passage is gradually exposed to the port conditions rather than adjusting instantaneously. This process is called gradual opening and the period of adjustment, wherein the leading and trailing walls of a rotor passage move out of a solid endwall, allowing the passage to be fully exposed to the inlet-port conditions, is herein referred to as the opening time. Under conditions of gradual opening, the formation of the shock wave and the evolution of the contact interface may be substantially altered.

Eidelman[2] presented a numerical simulation of gradual opening in wave rotor passages showing that the dynamics of the passage opening greatly modifies the flow pattern compared with that of instantaneous opening. The process of gradual opening was observed to distort the fluid interface in the passage-to-passage plane and lead to a finite time for the formation of shock or compression waves. These events can adversely affect the performance of a wave rotor. Since Eidelman's model was two dimensional it could not include the effects of Coriolis and centripetal accelerations brought on by the rotation of the passage.

For a given rotor passage geometry, the gradual opening time is inversely proportional to the rotational speed of the passage. Therefore, the problem of gradual opening is intrinsically coupled to that of rotation. Larosiliere and Mawid[3]

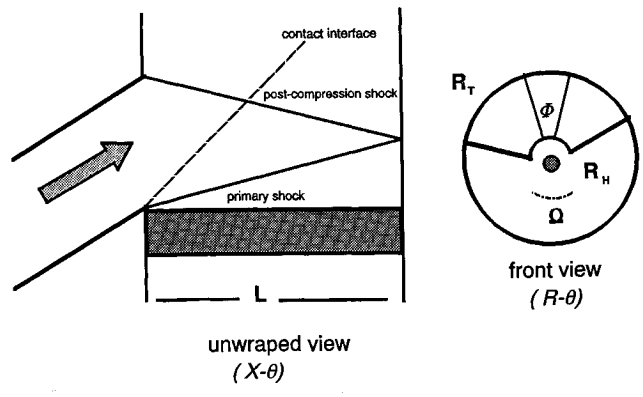

Fig. 1 Schematic representation of a wave rotor charging process.

have shown that the centripetal acceleration brought on by the rotation of a channel can significantly distort the fluid contact interface in a meridional plane. This implies the possibility of competition between the effect of gradual opening and that of rotation.

In the present study, a numerical simulation of the wave rotor charging process is performed to illustrate the impact of gradual opening accompanied by passage rotation. The three-dimensional inviscid flow equations, formulated in a rotating reference frame, are solved numerically for a single wave rotor passage. Variations in the response of the flowfield in a passage of fixed geometry are examined over a range of rotational speeds. A discussion of the results highlighting implications for wave rotor design is provided.

Formulation

The gradual opening problem involves a coupling between the inlet-port flow and the flow in the wave rotor passages. Flow through the port is for the most part steady,[1] but the flow in a wave rotor passage is unsteady and periodic in time. In the present study, the aim is not to provide a detailed description of the coupling between the inlet-port flow and the flow in the rotor passage, but rather to characterize the response of the flowfield in a rotating passage to the gradual application of the stationary inlet-port conditions. Thus, a single wave rotor passage is tracked as it passes stationary endwalls and the inlet port. The port flow is not calculated, however, its primary effect is accounted for through boundary conditions at the inflow plane.

Governing Equations

The geometry of the problem is illustrated in Fig. 1. It consists of a single cylindrical wave rotor passage of length L, and sector angle Φ. At $t = 0$, the passage is fully enclosed. Following this time, the solid-wall boundary conditions at the left side ($x = 0$) of the passage are gradually replaced with those of the inflow-plane as the passage rotates out of the endwall. The right side is always closed. Viscous effects and heat conduction are neglected.

A nondimensionalization of the geometry is obtained by scaling the axial coordinate with L, the circumferential coordinate with Φ, and the radial coordinate with R_T. Let (R, x, θ') denote a dimensionless cylindrical coordinate system attached to the rotor. The x axis lies along the axis of rotation and the rotating channel is restricted by the five walls: $\theta' = 0$, $\theta' = 1$, $R = R_H/R_T$, $R = 1$, and $x = 1$. The equations are made dimensionless by introducing a reference length L_{ref} for the gradient operator, a reference time τ, a reference density ρ_∞, and a reference speed of sound a_∞. Because there is as yet no obvious way to assign definite values to the reference quantities, they will be left unspecified for now.

Combinations of the reference scales are selected so that the following quantities, defined without asterisks, are dimensionless:

$$t = \frac{t^*}{\tau}, \qquad \rho = \frac{\rho^*}{\rho_\infty}, \qquad \boldsymbol{w} = \frac{\boldsymbol{w}^*}{a_\infty}, \qquad p = \frac{p^*}{\rho_\infty a_\infty^2}$$

$$E = \frac{E^*}{a_\infty^2}, \qquad \nabla = L_{\text{ref}}\nabla^*$$

The flow is modeled by the unsteady three-dimensional Euler equations[4] written in a rotating reference frame

$$B\frac{\partial \rho}{\partial t} + \nabla\cdot(\rho \boldsymbol{w}) = 0 \tag{1a}$$

$$B\frac{\partial \rho \boldsymbol{w}}{\partial t} + \nabla\cdot(\rho \boldsymbol{w}\boldsymbol{w}) + 2R_\Omega \rho \hat{\boldsymbol{e}}_\Omega \times \boldsymbol{w} - M_\Omega^2 \rho \nabla\left(\frac{R^2}{2}\right) = -\nabla p \tag{1b}$$

$$B\frac{\partial \rho E}{\partial t} + \nabla\cdot(\rho \boldsymbol{w} h_{tR}) = 0 \tag{1c}$$

completed by the perfect gas state relation

$$T = \gamma(p/\rho) \tag{1d}$$

where h_{tR} is the rothalpy

$$h_{tR} = [T/(\gamma - 1)] + \tfrac{1}{2}w^2 - \tfrac{1}{2}M_\Omega^2 R^2 \tag{1e}$$

and E is the total energy per unit mass in the rotating frame

$$E = h_{tR} - (p/\rho) \tag{1f}$$

Besides the ratios of geometric length scales (i.e., $\Phi R_T{:}R_T{:}L{:}L_{\text{ref}}$) implicitly contained in the gradient operator, the equations of motion depend on three other dimensionless parameters

$$B = \frac{L_{\text{ref}}/a_\infty}{\tau}$$

$$M_\Omega = \frac{\Omega R_T}{a_\infty}$$

$$R_\Omega = \frac{L_{\text{ref}}/a_\infty}{1/\Omega}$$

A proper scaling of the problem is required so that the relative importance of each term in the governing equations is indicated by these dimensionless parameters. Note that the wheel Mach number M_Ω already indicates the magnitude of the centrifugal force, but B and R_Ω demand further insights into the character of the problem. Boundary and initial conditions of the flow may be interrogated to define intrinsic reference scales of the problem.

Boundary Conditions

Boundary conditions at $x = 0$ are formulated by introducing a gate function $G(\theta)$ simulating the inlet-port opening and closing. An expression for the gate function is given as

$$G(\theta) = H(\theta - 1) - H(\theta - \theta_p) \tag{1g}$$

where $H(\theta)$ is Heaviside's unit step function, the angle θ is an absolute angle measured in the frame of the stationary port, and θ_p is the angular position of the port closing. A transformation from the absolute frame θ to the rotating frame θ' can be written as

$$\theta = \theta' + (\tau/\tau_o)t - (2\pi/\Phi)k \qquad 0 \le \theta' \le 1$$
$$k = 0, 1, 2, \ldots \tag{1h}$$

where $\tau_o = \Phi/\Omega$ is the passage opening time. The above expression assumes that the origins of the two reference frames coincide at $t = 0$. Introducing this transformation into Eq. (1g) gives an indication of whether a specific spatial location on the rotor passage at $x = 0$ corresponds to a solid endwall [$G(\theta') = 0$] or to the inflow-plane [$G(\theta') = 1$] at a given time. Inflow boundary conditions are discussed in the computational solution section. Free-slip velocity boundary conditions are applied at all solid walls, and wall pressures are obtained by solving the normal momentum equation.

Initial Conditions

At $t = 0$, the passage is assumed to contain a gas at rest relative to the closed passage walls. Uniform thermodynamic conditions are prescribed (i.e., $p = 1/\gamma$, $\rho = 1$). Although a radial variation of the thermodynamic properties can be prescribed by assuming homentropic solid-body rotation, this is

probably not necessary for the range of parameters to be considered. Nevertheless, the present initialization procedure is thought to closely approximate conditions in an actual rotor where the gas has been brought to rest through gasdynamic wave actions.

Scaling

For the sake of simplicity, the uniform thermodynamic reference state ∞ is taken to be that which exists in the passage at the initial time ($t = 0$). In deciding the reference length scale for the gradient operator and the reference time scale, attention should be focused on the region where and over what time period the dependent variables are changing most rapidly. It is anticipated that during the gradual opening period, most of the changes in the flowfield will occur over a distance on the order of the passage width. This implies that

$$B = \frac{\Phi R_T/a_\infty}{\tau_o} = M_\Omega, \qquad R_\Omega = \Phi M_\Omega, \qquad t \leq 1$$

After the gradual opening period, it is envisioned that the length of the passage and the longitudinal transport time, $\tau_L = L/a_\infty$, are the intrinsic reference scales over which rapid changes will occur. In this regime, the relevant parameters reduce to

$$B = \frac{L/a_\infty}{\tau_L} = 1, \qquad R_\Omega = (L/R_T)M_\Omega, \qquad t > \frac{\tau_o}{\tau_L}$$

For fixed geometry and boundary conditions, the governing equations are characterized by only one parameter, the wheel Mach number M_Ω. The wheel Mach number has three different interpretations. First, it gives a measure of the relative strength of the centripetal acceleration. Second, during the gradual opening transient, the wheel Mach number can also be interpreted in terms of the ratio of the wave transport time across the width of the passage ($\Phi R_T/a_\infty$) to the passage opening time. Therefore, for fixed geometry and inlet conditions, increasing the wheel Mach number reduces the opening time compared with the wave transport time across the passage width. This implies less wave reflections during the gradual opening time period. Third, M_Ω gives a measure of the deformation of the interface in terms of the ratio of tangential ($\sim t$) to longitudinal ($\sim t/M_\Omega$) extent of the interface during the gradual opening period. Moreover, the effects of Coriolis acceleration on the fluid contact interface, when they exist, will tend to be more pronounced with increasing wheel Mach number.

Computational Scheme

A two-stage Runge-Kutta algorithm was used to numerically solve the governing equations. This scheme employs explicit time-marching along with central difference spatial discretization on a boundary-fitted H-mesh. The local truncation error is formally second-order both in space and time. A blend of second- and fourth-difference artificial dissipation terms incorporating a density gradient switch is added to capture discontinuities and to control nonlinear instabilities. Further details concerning implementation of this scheme can be found in Ref. 5. The treatment of the inflow boundary follows.

The base flow at the inflow-plane ($x = 0$) can be expressed as the sum of two components: 1) a steady flow and 2) an unsteady perturbation. This flow is assumed to evolve from the steady inlet-port flow, which is partially specified and partially computed from the solution interior to the rotor passage. It is this interior solution that is responsible for the unsteady perturbation. In addition, the base flow is assumed to be isentropic. At the inflow-plane, the procedure adopted for describing the base flow consists of prescribing the incoming waves and using characteristic relations to supply the outgoing waves (see, e.g., Thompson[6] for more details).

At each point on the inflow boundary four pieces of information must be furnished to calculate the flow variables. If the upstream axial Mach number is always subsonic, the Riemann invariant along the downstream running characteristic, the relative tangential velocity, the radial velocity, and the upstream entropy are specified. The Riemann invariant along the upstream running characteristic is extrapolated from the interior. This procedure allows all of the flow variables to be updated along the inflow boundary.

Results and Discussion

A fixed passage geometry with a length-to-width ratio $L/(R_T\Phi) = 11.6$, a hub-to-tip radius ratio $R_H/R_T = 0.934$, and a length-to-tip radius ratio $L/R_T = 1.0$ was used. The uniform computational mesh consisted of 500 longitudinal nodes, 30 radial nodes, and 30 circumferential nodes. Uniform inflow-plane conditions having a downstream running Riemann invariant $J^+ = 7.08$, upstream entropy $p/T^{\gamma/(\gamma-1)} = 0.126$, and zero circumferential and radial relative velocity components ($w_\Theta = 0$, $w_R = 0$) were assumed. These conditions are typical for a wave rotor passage filled with a quiescent charge of air and encountering a perfectly matched (i.e., zero incidence to the rotor) inlet port supplying hot, high-pressure driver gas. The inflow-plane conditions are held fixed along with a specific heat ratio $\gamma = 1.4$.

To assess the accuracy and fidelity of the simulation, an instantaneous opening case with zero rotation was run as a baseline for comparison. This is a one-dimensional problem with an exact analytical solution. The usual difficulty in finite difference computations is that the numerical diffusion required for stability often overwhelms the actual physical diffusion. Thus, it is difficult to capture strong gradients without smearing fine details of the flow. The results to be presented feature calibrated artificial dissipation parameters selected to minimize the numerical diffusion, with a time step determined by a Courant condition (CFL = 0.5). Figure 2 shows a comparison of the numerical results with the exact one-dimensional Riemann solution. The shock and contact are resolved in four and nine mesh points ($\Delta x = 1/499$), respectively. An acceptable level of accuracy can be observed.

The adequacy of the 500 × 30 × 30 mesh was checked for the case of an oblique discontinuity by comparing results among computations with reduced grid spacings in all three coordinate directions. No significant differences (i.e., less than 5% change in density and pressure distributions) in the structure of the interface were observed with more refined grids (600 × 30 × 30, 500 × 50 × 30, 500 × 30 × 50). Parameter ranges for the simulation are given in Table 1. Also listed in Table 1, are the ratios of full passage opening time τ_o to longitudinal transport time τ_L.

Gradual Opening Transient Response

The transient response of the flowfield in the passage to the gradual opening process is illustrated in Fig. 3 through density contours in a passage-to-passage plane (i.e., $x - \theta'$) at midheight for several wheel Mach numbers and other parameters as given in Table 1. Two instants during the gradual opening transient are presented, specifically, the times when the passage is half opened ($t = 0.5$) and fully opened ($t = 1.0$).

As the passage gradually opens, a series of curved compression waves followed by a contact interface, as shown in Fig. 3a, emanate from the small opening. The waves penetrate into the passage and reflect from the trailing wall to interact with other incoming compression waves and with the interface. For $Mo = 0.1$, a large clockwise-oriented vortex is observed. Part of the interface wraps around this vortex and assumes a spiral configuration.

It can be seen in Fig. 3 that the interface evolution during the gradual opening period exhibits increasing distortion. This distortion is caused by two mechanisms: 1) dilatation of fluid elements comprising the interface, and 2) generation of vor-

ticity (i.e., local rotation of fluid elements) by the actions of baroclinic torques. Interaction of the reflected waves with the interface produces baroclinic vorticity (i.e., $\nabla\rho \times \nabla p$), as suggested by the winding of the interface. If the opening time were instantaneous, the interface would be a planar surface normal to the leading and trailing walls of the passage, but due to the kinematics of gradual opening, the interface is stretched.

The higher the wheel Mach number, the smaller the deformation as previously discussed. For $Mo = 0.1$, a portion of the interface acquires a quasiplanar orientation extending across the passage width similar to that with instantaneous opening, followed by a trailing portion that wraps around a spiral vortex. The orientation of this spiral is consistent with the sign of baroclinic vorticity production due to wave reflections from the trailing wall. A similar but less developed interfacial structure is observed for $Mo = 0.3$. In contrast, the $Mo = 0.5$–0.7 cases experience a much smaller deformation with no evidence of a spiral configuration. It can be inferred from the above considerations that whether a fully developed spiral vortex occurs during or after the gradual opening period depends on the wheel Mach number. Thus, for fixed geometry and port conditions, the wheel Mach number is the governing parameter that dictates the response of the interface during the gradual opening process.

Kinematics of Interface and Shock

The evolution of the interface and the propagation of compression or shock waves are shown in Fig. 4 through density contours in a passage-to-passage plane at midheight for wheel Mach numbers $Mo = 0.3$ and 0.7. Note that the dimensionless times are based on the longitudinal transport time scale τ_L. The plots clearly show the multiple wave reflections from both the leading and trailing walls of the passage. Increasing the wheel Mach number is seen to reduce the number of wave reflections that occur before the passage is fully opened. This explains the interface configurations shown in Fig. 3 and the subsequent delay in the shock formation process. With instantaneous opening (Fig. 2), the shock has traversed more than half (i.e., $x = 0.6$) of the passage length at $t = 0.5$, whereas for $Mo = 0.3$ and 0.7 the shock or compression waves have barely penetrated midpassage length. At $t = 1.0$, the postcompression shock is traveling to the left and begins interacting with the interface at $t = 1.5$.

Figure 4 also shows that stretching of the interface due to the kinematics of gradual opening quickly dies out after the passage is fully opened. However, the spiraling caused by vorticity production grows as the interface evolves. Interac-

Table 1 Simulation parameters (CFL = 0.5)

M_Ω, M_o	τ_o/τ_L	R_Ω (based on $R_T\Phi$)	R_Ω (based on L)
0.1	0.860	0.0086	0.100
0.3	0.287	0.0258	0.300
0.5	0.172	0.0413	0.500
0.7	0.123	0.0600	0.700
1.0	0.086	0.0860	1.000

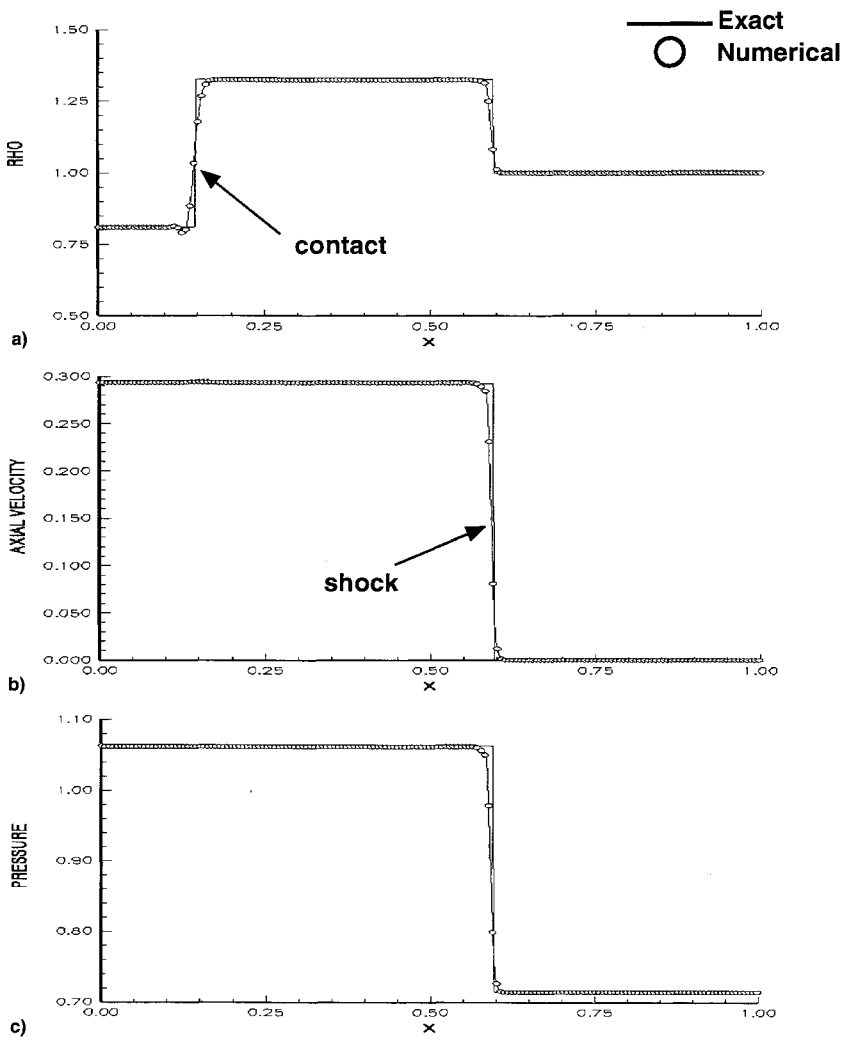

Fig. 2 Comparison of computed baseline case having instantaneous opening and zero rotation with exact one-dimensional Riemann solution, $t = 0.5$: a) density, b) axial velocity, and c) pressure.

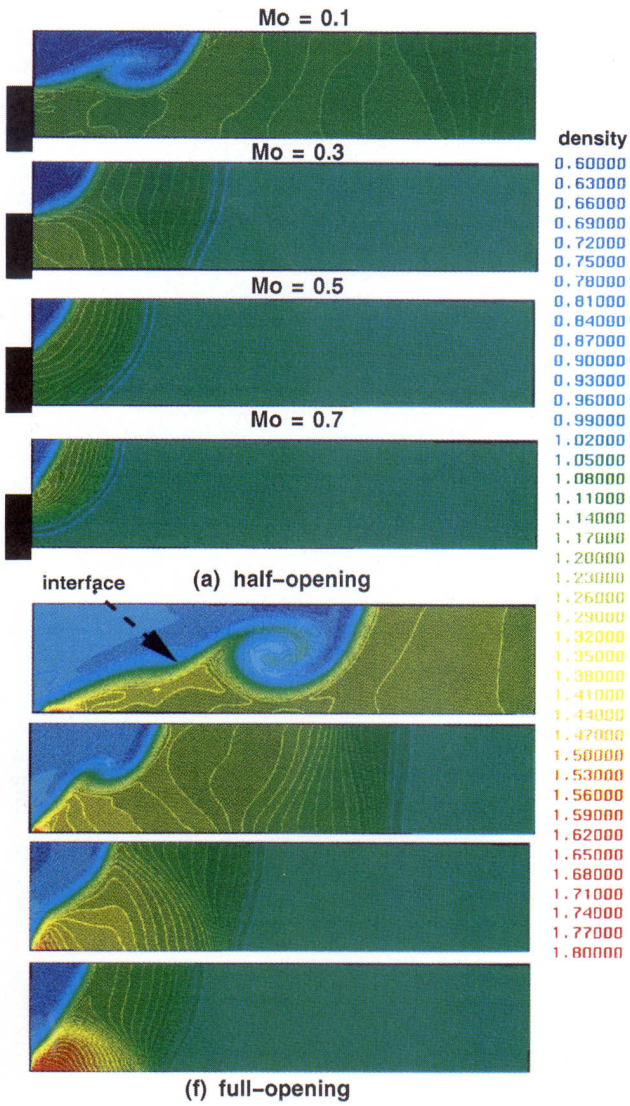

Fig. 3 Density contours for different wheel Mach numbers in a passage-to-passage plane at midheight during the gradual opening process.

tion of the shock with the interface can be observed to further deform the interface. At $t \geq 1.5$, the spiral has diminished somewhat and the interface is spreading along the leading wall for $Mo = 0.7$. Interrogation of the full three-dimensional flowfield suggests that this is caused by spanwise migration of fluid elements along the interface as a result of Coriolis accelerations.

Meridional Plane Distribution

The development of the interface is illustrated in Fig. 5 at a time after completion of the postcompression process ($t \geq 2.0$). Circumferentially averaged density ($\int \rho \, d\theta'$) distributions in a meridional plane are shown for wheel Mach numbers $Mo = 0.1, 0.5, 1.0$. The instantaneous opening with zero rotation case is included as a baseline.

For $Mo = 0.1$, there is little radial variation in the density distribution except for a small radially attenuated hump. It is conjectured that this hump is a result of Coriolis accelerations induced by the passage-to-passage vortex generated during the gradual opening transient. However, for $Mo \geq 0.5$, a well-defined radial skewing of the interface can be observed. The radial distortion is caused by baroclinic vorticity generated through the action of centripetal acceleration at the interface.

Both the gradual opening process and passage rotation result in the generation of circulatory flows near the interface.

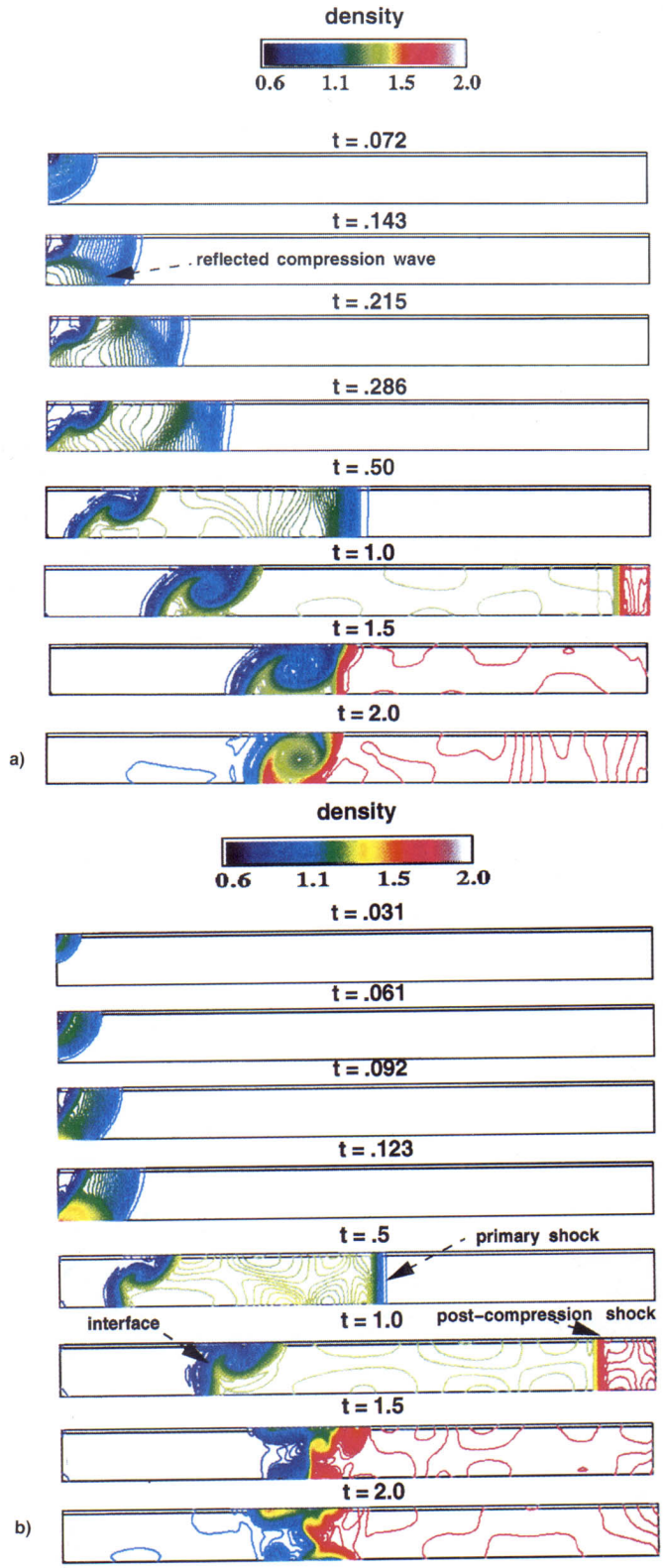

Fig. 4 Evolution of density field in a passage-to-passage plane at midheight for Mo = a) 0.3 and b) 0.7.

According to Kelvin's theorem, the relative circulation evolves for ideal flows as

$$B \frac{\partial \Gamma}{\partial t} + \boldsymbol{w} \cdot \nabla \Gamma = \oint T \, ds - 2R_\Omega \oint \hat{e} \times \boldsymbol{w} \cdot d\boldsymbol{x} \qquad (2)$$

This expression shows how the relative circulation changes along particle paths due to reversible heat transfer and work

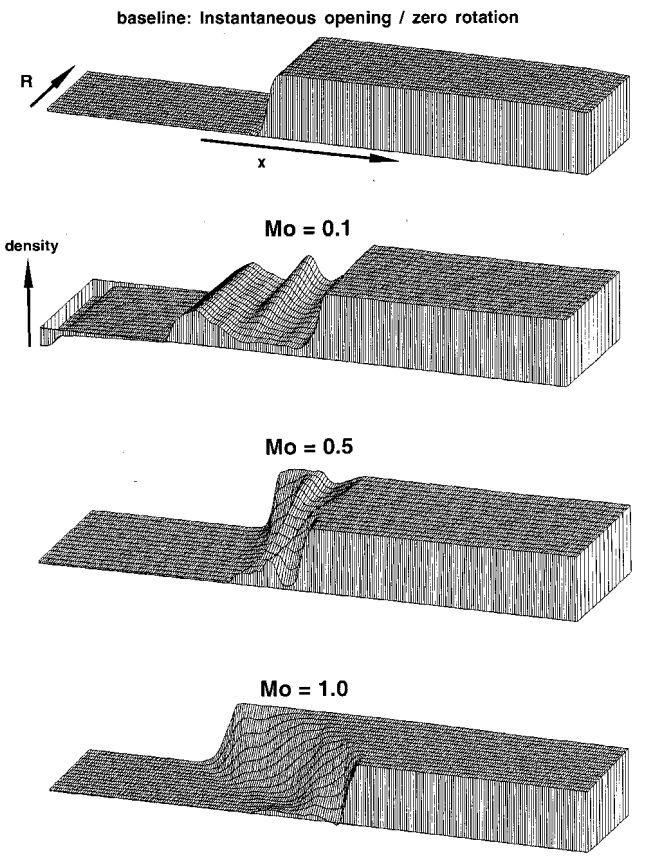

Fig. 5 Circumferentially averaged density distribution in a meridional plane after postcompression, $t = 2.0$.

done by Coriolis forces. The reversible heat transfer has two origins: 1) interaction of reflected compression waves with the interface and 2) evolution of the interface in a radially stratified medium generated by the centripetal acceleration. For instantaneous opening without any rotation, the relative circulation is constant in time with the constant being zero. With gradual opening and passage rotation, circulation is produced at the interface depending on the temperature nonuniformity and the entropy change. This circulation is the cause of the radial skewing of the interface observed in Fig. 5. Note also that Coriolis forces can act either as a compensating or a destabilizing mechanism on the production of circulatory flows.

Wave Rotor Design Implications

Similar to the results of Eidelman,[2] reducing the opening time (i.e., increasing Mo) for a fixed geometry allows a more rapid shock formation and propagation. The time for shock formation is significantly greater than that with instantaneous opening. This has strong implications for port timing and wave arrangement. Furthermore, the distortion of the contact interface created by circulatory flows varies in a nonlinear fashion with opening time or wheel Mach number. The interface distortion may lead to mixing between the two streams participating in the energy transfer.

Since there are no dissipative mechanisms in the results presented, it is not possible to quantify a mixing loss in the strict sense of the word. However, Eq. (2) and Fig. 5 suggest that the distortion of the interface because of circulatory flows and gradual opening can be interpreted in terms of availability of a uniform volume of compressed fluid. A postcompression volumetric efficiency is defined as the ratio of available uniform volume of fluid to that for the baseline case with instantaneous opening and zero rotation. Thus, a measure of

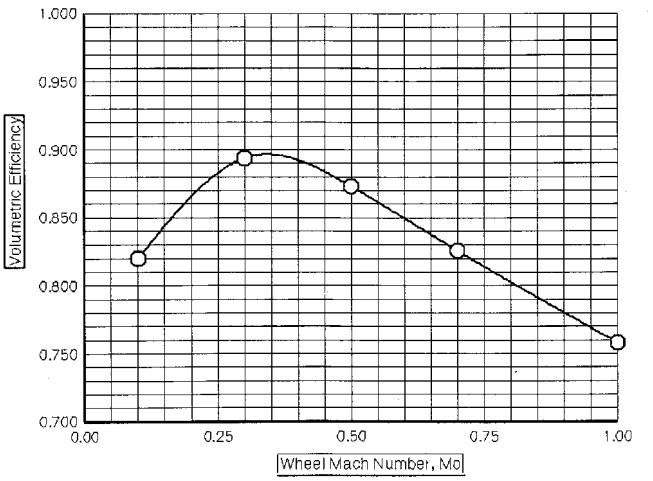

Fig. 6 Variation of postcompression volumetric efficiency with wheel Mach number.

the relative effects of gradual opening and passage rotation is given by

$$\eta_V = (V/V_0)$$

where V_0 is the available volume of compressed fluid after postcompression under conditions of instantaneous opening and zero rotation. Figure 6 shows the variation of η_V with wheel Mach number for the conditions presented herein. The optimum wheel Mach number appears to be about $Mo = 0.3$–0.4. For lower wheel Mach numbers, the effects of gradual opening are prevalent. When Mo is increased beyond the optimum, the adverse effects of centripetal and Coriolis accelerations become dominant.

Summary

A numerical simulation of the three-dimensional, inviscid flow dynamics during the wave rotor charging process under conditions of gradual opening accompanied by rotation provides insight into the evolution of the contact interface. For fixed geometry and boundary conditions, the response of the interface depends on the wheel Mach number. At low wheel Mach numbers (i.e., $Mo < 0.3$), or long opening times, the interface between in-flowing driver gas and the driven gas in the passage becomes very distorted due to stretching caused by the kinematics of gradual opening and baroclinic vorticity generated by interactions of the interface with multiple reflected compression waves. For higher wheel Mach numbers (i.e., $Mo \geq 0.3$), or short opening times, the interface is less deformed and the vorticity generation by the interaction of reflected waves with the interface is reduced. However, the larger centripetal acceleration with increasing wheel Mach number generates additional vorticity that causes a three-dimensional interface distortion.

The development of the wave system is also dependent on the wheel Mach number or passage opening time. For low wheel Mach numbers or longer opening times, a substantial time period is required for the formation of shocks. Due to the highly distorted interface, subsequent interaction of the reflected shock with the interface may result in the creation of a complex flow pattern.

It can be concluded that the gradual opening process and the influence of rotation on the flow patterns are intimately coupled. This should be kept in mind during the wave rotor design process, not only for proper port-timing and wave arrangement, but also because of the losses that may occur due to mixing and wave reflections. Rotating faster in order to reduce the adverse effects of gradual opening may create other deleterious effects due to Coriolis and centripetal ac-

celerations. The results presented herein can help guide the designer in achieving an optimum compromise.

References

[1]Shreeve, R. P., and Mathur, A. (eds.), *Proceedings of the 1985 ONR/NAVAIR Wave Rotor Research and Technology Workshop*, pp. 9–49, 86–115 (NPS-67-85-008).

[2]Eidelman, S., "The Problem of Gradual Opening in Wave Rotor Passages," *Journal of Propulsion and Power*, Vol. 1, No. 1, 1985, pp. 23–28.

[3]Larosiliere, L. M., and Mawid, M., "Analysis of Unsteady Wave Processes in a Rotating Channel," AIAA Paper 93-2527, July 1993.

[4]Vavra, M. H., *Aero-Thermodynamics and Flow in Turbomachines*, Wiley, New York, 1960.

[5]Chima, R. V., and Yokota, J. W., "Numerical Analysis of Three-Dimensional Viscous Internal Flows," *AIAA Journal*, Vol. 28, No. 5, 1990, pp. 798–806.

[6]Thompson, K. E., "Time-Dependent Boundary Conditions for Hyperbolic Systems, II," *Journal of Computational Physics*, Vol. 89, 1990, pp. 439–461.